



Dedicated to innovation in aerospace

NLR-TP-2019-202 | October 2019

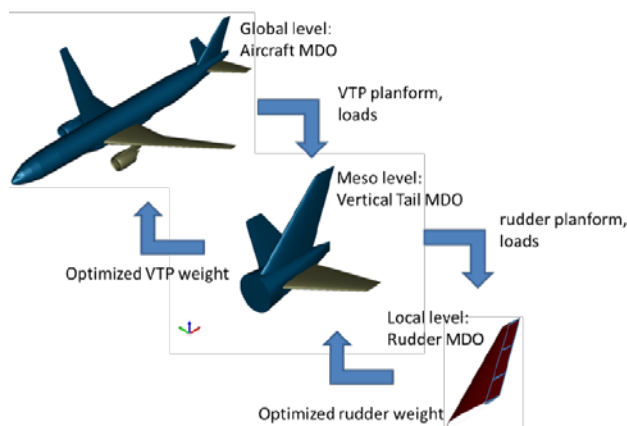
# A collaborative design method for the aircraft supply chain: multi-level optimization

CUSTOMER: European Commission



NLR – Netherlands Aerospace Centre

# A collaborative design method for the aircraft supply chain: multi-level optimization



*Example design optimization in a typical collaborative supply chain: rudder optimization on aircraft global level, vertical tail meso level and rudder local level*

## Problem area

Modern aircraft are highly advanced technological and competitive products that are developed by many multidisciplinary teams of experts from different companies, usually located in several countries. To reduce aircraft development costs, to reduce lead times and to establish a more competitive supply chain, aircraft Original Equipment Manufacturers (OEMs) need to incorporate at an early stage in the design process the influence of various disciplines on the overall design performance. In particular there is a need for efficient methods to address the problem of design optimization on aircraft level as well as subsystem level.

## Description of work

In the AGILE project, advanced technologies for optimization, multi-disciplinary collaboration and knowledge-enabled engineering have been developed and applied to preliminary aircraft design in various representative use cases. A multi-level optimization (MLO) approach has been applied to a collaborative

**REPORT NUMBER**  
NLR-TP-2019-202

**AUTHOR(S)**  
A.J. de Wit  
W.F. Lammen  
H.S. Timmermans  
W.J. Vankan  
D. Charbonnier  
T. van der Laan  
P.D. Ciampa

**REPORT CLASSIFICATION**  
UNCLASSIFIED

**DATE**  
October 2019

**KNOWLEDGE AREA(S)**  
Computational Mechanics and Simulation Technology  
Aerospace Collaborative Engineering and Design

**DESCRIPTOR(S)**  
Multidisciplinary Design Optimisation (mdo)  
Collaborative Engineering Optimization  
response surface method  
rudder

design problem of subcomponent-component-airframe design of an aircraft rudder. This problem was solved with a nested MLO. This nested optimization, including the rudder design tools, has been described in NLR-TP-2017-370. Furthermore, a two-level component-airframe design problem has been solved via multi-level optimization, as described in NLR-TP-2018-010. In the present report, the rudder design problem is specified as a three level optimization problem that is solved by applying a multi-level optimization strategy called Analytical Target Cascading (ATC).

## Results and conclusions

The ATC method and nested optimization method both arrive at the same design optima. However, in the case of ATC the number of communication events between the local-meso-global level becomes smaller than with the nested approach, in which the meso and local optimization are part of the global objective function. Limiting the amount of interaction is essential in order to create an efficient collaboration between the aircraft OEM (performing the global optimization) and the suppliers (performing the meso and local optimizations). As a result, using MLO the OEM and suppliers are able to significantly reduce the development time of an aircraft subsystem.

## Applicability

The MLO approach described in this work can be used between OEM and suppliers - including the Dutch aircraft industry - to reduce development time of an aircraft as well as subsystems.

### GENERAL NOTE

This report is based on a presentation held at the AIAA Aviation 2018 conference, Atlanta, 25<sup>th</sup>-29<sup>th</sup> June 2018.

### NLR

Anthony Fokkerweg 2  
1059 CM Amsterdam, The Netherlands  
p ) +31 88 511 3113  
e ) info@nlr.nl i ) www.nlr.nl



Dedicated to innovation in aerospace

NLR-TP-2019-202 | October 2019

# A collaborative design method for the aircraft supply chain: multi-level optimization

CUSTOMER: European Commission

## AUTHOR(S):

A.J. de Wit	NLR
W.F. Lammen	NLR
H.S. Timmermans	NLR
W.J. Vankan	NLR
D. Charbonnier	CFS Engineering
T. van der Laan	GKN Fokker Aerostructures
P.D. Ciampa	DLR

This report is based on a presentation held at the AIAA Aviation 2018 conference, Atlanta, 25<sup>th</sup>-29<sup>th</sup> June 2018.

*The contents of this report may be cited on condition that full credit is given to NLR and the authors.  
This publication has been refereed by the Advisory Committee AEROSPACE VEHICLES (AV).*

<b>CUSTOMER</b>	European Commission
<b>CONTRACT NUMBER</b>	636201
<b>OWNER</b>	European Commission
<b>DIVISION NLR</b>	Aerospace Vehicles
<b>DISTRIBUTION</b>	Unlimited
<b>CLASSIFICATION OF TITLE</b>	UNCLASSIFIED

<b>APPROVED BY:</b>		<b>Date</b>
<b>AUTHOR</b>	A.J. de Wit	27-09-2019
<b>REVIEWER</b>	E. Baalbergen	27-09-2019
<b>MANAGING DEPARTMENT</b>	A.A. ten Dam	30-09-2019

# Contents

<b>Nomenclature</b>	<b>4</b>
<b>I. Introduction</b>	<b>6</b>
<b>II. The rudder design case</b>	<b>7</b>
A. Rudder MLO problem formulation	8
B. Aircraft and Rudder design analysis tools	9
C. High fidelity analysis of the rudder	11
<b>III. Surrogate modelling and nested optimization</b>	<b>12</b>
A. Surrogate models derived from the analysis tools	12
B. Aircraft rudder optimization results with the surrogate models	15
<b>IV. MLO process via concept of Analytical Target Cascading (ATC)</b>	<b>167</b>
<b>V. Conclusions</b>	<b>24</b>
<b>Funding Sources</b>	<b>25</b>
<b>Acknowledgments</b>	<b>25</b>
<b>References</b>	<b>25</b>

# A collaborative design method for the aircraft supply chain: multi-level optimization

A.J. de Wit\*, W.F. Lammen<sup>†</sup>, H. Timmermans<sup>‡</sup> and W.J. Vankan<sup>§</sup>  
NLR - Netherlands Aerospace Centre, Postbus 90502, 1006 BM, Amsterdam, the Netherlands

D. Charbonnier<sup>¶</sup>  
CFS Engineering, EPFL Innovation Park, Bât. A, 1015 Lausanne, Switzerland

T. van der Laan<sup>||</sup>  
GKN Fokker Aerostructures, P.O. Box 1, 3350 AA, Papendrecht, the Netherlands

P.D. Ciampa<sup>\*\*</sup>  
DLR - German Aerospace Center, Hein-Saß-Weg 22, 21129, Hamburg, Germany

In the AGILE project, advanced technologies for optimization, multi-disciplinary collaboration and knowledge-enabled engineering are developed and applied to conceptual and preliminary aircraft design. Various representative use cases of some conventional and unconventional aircraft configurations are considered. This paper describes the application of a multilevel optimization (MLO) strategy based on analytical target cascading (ATC) to a use case of rudder design on a conventional aircraft configuration. As a reference a traditional nested optimization method is applied as well. Both methods arrive at the same design optima. In the case of ATC the amount of interaction between the global and the local level optimizations is reduced. The MLO is demonstrated by applying surrogate models that were derived from aircraft and rudder design analyses performed by the partners in the AGILE project. The rudder design case illustrates that applying MLO provides insight into the coupled design problem both for the aircraft OEM and for the supplier. Development time is reduced by minimizing the number of interaction events, providing a common understanding of the design problem, establishing interfaces in the design process and therefore reducing the risk of late design changes.

## Nomenclature

$\cdot$	= element by element multiplication of vectors
$\overline{\dots}$	= design variable upper bound
$\underline{\dots}$	= design variable lower bound
$\pi$	= penalty function
$\tau$	= Consistency error tolerance
$\tau_{ATC}$	= Objective change tolerance
$\alpha$	= weights
$\beta$	= penalty incrementation factor
$C$	= consistencies
$R$	= responses
$T$	= targets

\*R & D Engineer, Collaborative Engineering Systems Department

<sup>†</sup>R & D Engineer, Collaborative Engineering Systems Department

<sup>‡</sup>R & D Engineer, Flight Physics Department

<sup>§</sup>Senior Scientist, Collaborative Engineering Systems Department

<sup>¶</sup>Senior Scientist

<sup>||</sup>Knowledge Engineering Specialist

\*\*Team Lead MDO

$v$	=	Lagrange multipliers
$w$	=	penalty parameters
$b$	=	span
$c$	=	chord
$f$	=	objective function
$F$	=	Force
$h$	=	output rudder design tool
$\kappa$	=	scaling factor
$m$	=	mass
AML/AMLoad	=	Aeroelastic Modelling and Loads analysis tool
ATC	=	Analytical Target Cascading
CFD	=	Computational Fluid Dynamics
DoE	=	Design of Experiment
FEM	=	Finite Element Method
HDOT	=	Hinge-System Design and Optimization Tool
HTP	=	Horizontal Tail Plane
LHS	=	Latin Hypercube sampling
MDO	=	Multi-Disciplinary Design and Optimization
MLO	=	Multi-Level Optimization
OAD	=	Overall Aircraft Design
OEM	=	Original Equipment Manufacturer
RMSE	=	Root Mean Square Error
SQP	=	Sequential Quadratic Programming
VTP	=	Vertical Tail Plane
Subscripts		
fuel	=	aircraft fuel
g	=	global
l	=	local
m	=	meso
obj	=	objective
rud	=	rudder
sc	=	scaling
MaxFuel	=	maximum fuel mass

## I. Introduction

MODERN aircraft are highly advanced technological and competitive products that are developed by many multi-disciplinary teams of experts from different companies, often located in several countries. The design and development is a complex collaborative process that involves an extended supply chain. Within this supply chain a distinction is made between the aircraft Original Equipment Manufacturer (OEM) and the suppliers of (sub)systems and components. Each supplier is responsible for its own (sub)system design. The OEM is responsible for the overall aircraft design and the interfacing between the overall aircraft and the (sub)systems.

Dividing the design process of an aircraft (sub)system via interfaces of collaboration and data exchange between OEM and suppliers has the advantage of allowing (sub)system suppliers to advance in their specific expertise separately from the OEM. From a supplier perspective, this decomposition may lead to an optimal (sub)system design. However, from an OEM perspective it may result in a non-optimal overall aircraft design.

To optimize the overall aircraft in an integrated way and avoid costly redesign iterations it is necessary to simultaneously optimize the overall aircraft and its (sub)systems. This paper demonstrates a Multi-Level Optimization (MLO) method to integrate the local level (sub)system design optimization within the global level overall aircraft design optimization. A use case of aircraft rudder design is considered representing a sub-system design of a rudder within the system design of a vertical tail plane (VTP)\* within the overall aircraft design. The three level hierarchy of the overall aircraft level, to vertical tail system and the rudder sub-system level and the coupling between the levels is embedded in the design problem.

The paper is organized as follows:

- Section II formulates the rudder design optimization problem.
- Section III introduces surrogate modeling to the aircraft analysis and rudder design tools in a Multi-disciplinary Design Optimization (MDO) context.
- Section IV describes an MLO method based on Analytical Target Cascading (ATC) and applies it to the rudder design optimization problem.
- Section V presents the main conclusions.

---

\*Here, VTP is including the rudder.

## II. The rudder design case

An MLO test case for integrated component-airframe design optimization has been defined by GKN Fokker, one of the industrial partners in AGILE, who is a supplier of aircraft structural components to aircraft OEMs. The rudder design is based, among others, on the rudder geometric specifications (e.g. rudder chord, span) and the applicable rudder loads (e.g. rudder aerodynamic forces, hinge forces).

Both planform specifications and applicable rudder loads are provided by the aircraft OEM. The rudder loads are a consequence of the prescribed certification load cases (see CS 25.147 [1]). One such certification load-case for rudder design is “Flying with one engine inoperative”. In this case the rudder needs to be able to compensate the yaw moment of the aircraft resulting from asymmetric thrust caused by one engine being inoperative, see Figure 1.

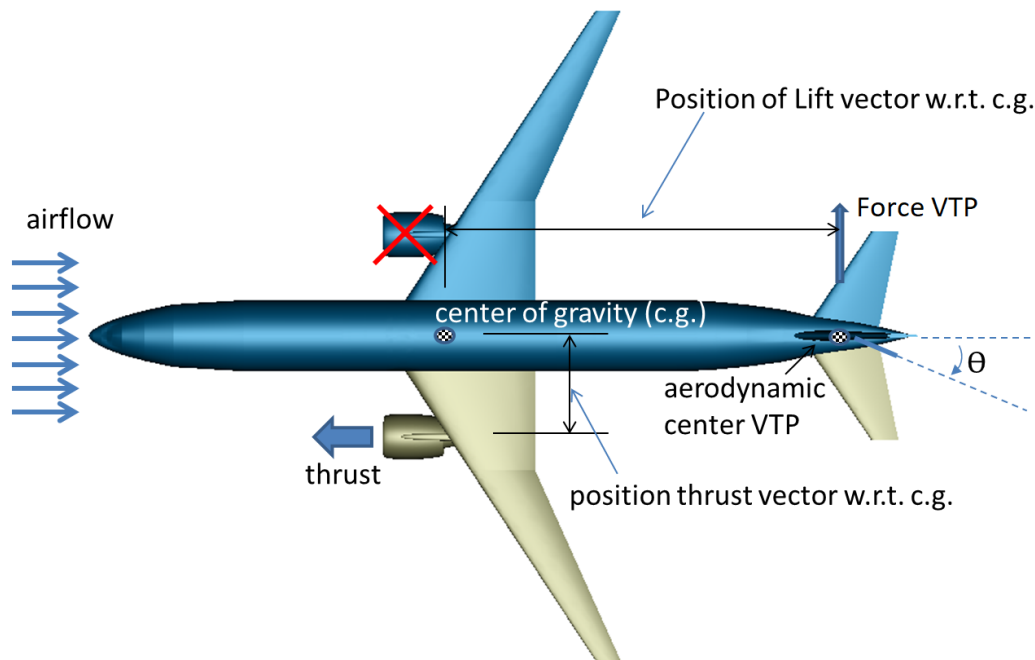


**Fig. 1 Yaw moment caused by asymmetric thrust. The case illustrated here is due to a twin-engine aircraft loosing one engine’s thrust.**

For larger aircraft the tail assembly is outsourced to a supplier that manufactures and/or assembles the empennage. For the use case considered in this paper a simplification is made and only the VTP section (vertical tail assembly) is assumed to be outsourced to a separate manufacturer. In addition, the rudder is assumed to be provided by another supplier and integrated by the VTP manufacturer. In this case, the rudder planform and applied loads are transferred from the VTP supplier to the rudder supplier.

On the level of the rudder structural design, the rudder structure is optimized for weight and cost, under the constraints that the requirements on specifications and loads are fulfilled. On the level of the VTP design, the tail structure can be optimized, e.g. for weight and/or cost using the VTP span and chord as design variables. On the level of the aircraft design, the whole aircraft structure is optimized, e.g. for weight and/or drag, using the main wing planform parameters as design variables.

In previous work the rudder design case was analyzed using a nested approach [2]. Optimization of aircraft and rudder level was done all-in-one using surrogate models that were built from input and output data of the design analyses. Hence, no use of the embedded hierarchy in the design problem was used. In a follow-up work the rudder design case was optimized using a two level hierarchy, see [3]. The rudder optimization and aircraft level optimization were solved using an MLO methodology named Analytical Target Cascading [4]. The present work extends this two-level hierarchy to a three-level hierarchy in which the Vertical Tail Plane (VTP) design is introduced as a meso-level.

The present study is a simplified version of an aircraft, VTP and rudder design case. This MLO use case is considered to demonstrate the essence of the approach. The MLO problem is further elaborated in Section II.A. A variation at aircraft level design is limited to the main wing span as design variable. In addition, a span-wise position of the engine

fixed at a percentage of the wing span is assumed and a constant thrust is assumed for the load case. This way, for the “one-engine-inoperative” load case an increase in wing span has a direct effect on the required rudder force due to the larger yaw moment. In addition, the rudder chord may need to be changed if the rudder deflection angle reaches its maximum when compensating the aircraft yaw moment.

On the level of the VTP design, the vertical tail mass is optimized for the loads corresponding to the “one-engine-inoperative” case. The VTP span is adjusted to minimize weight subjected to bounds on coupling variables that couple the optimization to the global and local level. A change in VTP may influence the weight and balance of the overall aircraft. In addition, changes in VTP design have an effect on the rudder planform.

On the level of the rudder design, the rudder mass is optimized for the loads corresponding to the “one-engine-inoperative” case. Furthermore, manufacturing constraints are considered to arrive at a rudder design. A change in rudder design may impact the VTP design and the interface between VTP and supplier. Furthermore, rudder changes may impact the overall aircraft design. For example, a change in rudder weight has an effect on the VTP weight and balance. A change in VTP has an effect on overall aircraft weight balance. This interaction is illustrated in Figure 2.

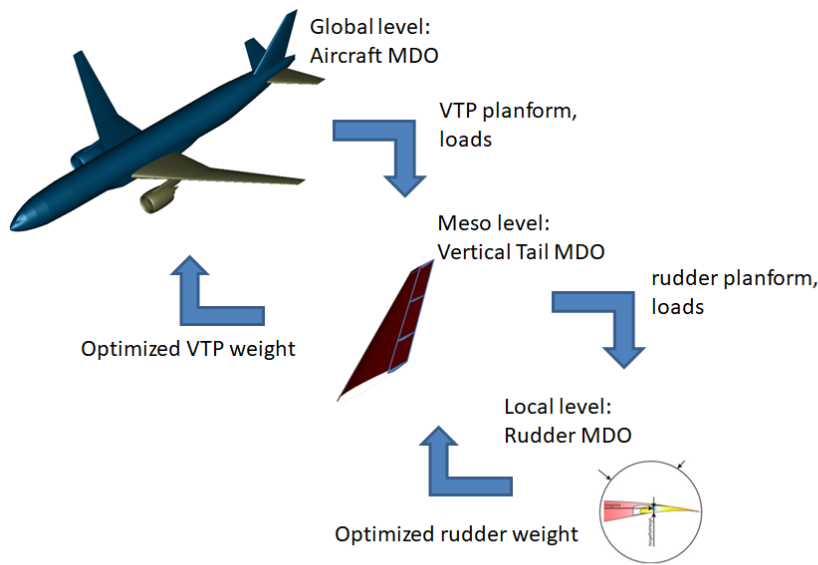


**Fig. 2** Global, meso and local levels in aircraft, Vertical Tail Plane and rudder design.

### A. Rudder MLO problem formulation

Mathematically, the aircraft rudder MLO use case can be formulated as follows. To demonstrate the essence, the number of design variables is kept to a minimum.

Assume that  $f_g(b_{wing}, m_{VTP})$  is some global aircraft optimization objective that depends on the global design variable wing span  $b_{wing}$  and in some way on the VTP mass  $m_{VTP}$ . The objective function  $f$  is typically chosen to improve aircraft level behavior, e.g. minimize aircraft weight, drag or fuel burn. Each of these parameters depends on the aircraft level variables, e.g. VTP weight or wing span. Assume that the VTP mass depends on the VTP planform, represented via VTP span ( $b_{VTP}$ ) and the rudder mass. Furthermore, due to stability requirements during various load cases of the aircraft (e.g. yaw moment) the VTP span increases with increasing wing span. The dependency of VTP span on wing span is:

$$b_{VTP} = b_{VTP}(b_{wing}) \quad (1)$$

and the VTP mass is mathematically expressed as:

$$m_{VTP} = m_{VTP}(b_{VTP}, m_{rud}) \quad (2)$$

The rudder mass  $m_{rud}$  depends on the rudder planform, represented via rudder span  $b_{rud}$  and rudder chord  $c_{rud}$  (design variable) and on the (resulting) rudder force (representing the loads) for which it has been designed. This is

mathematically expressed as:

$$m_{rud} = m_{rud}(c_{rud}, F_{rud}, b_{rud}) \quad (3)$$

with  $b_{rud} = 0.90b_{VTP}$ , rudder chord  $c_{rud}$  and rudder force  $F_{rud} = F_{rud}(c_{rud}, b_{wing})$ , assuming that the rudder force depends both on the rudder chord (representing the rudder planform) and the wing span (as explained earlier). Then the global aircraft level optimization problem is formulated as follows:

$$\begin{aligned} & \min_{b_{wing}, c_{rud}} && f_g(b_{wing}, m_{VTP}) \\ & \text{subject to:} && g(b_{wing}, c_{rud}) \leq 0 \\ & \text{bounded by:} && \underline{b}_{wing}, \underline{c}_{rud} \leq b_{wing}, c_{rud} \leq \bar{b}_{wing}, \bar{c}_{rud} \end{aligned} \quad (4)$$

With  $g$  a (nonlinear) constraint function that could be based on the maximum rudder deflection in combination with the applicable load case,  $\underline{b}_{wing}, \underline{c}_{rud}$  lower bounds and  $\bar{b}_{wing}, \bar{c}_{rud}$  upper bounds on the design variables.  $m_{VTP}$  has a dependency on  $c_{rud}$ , following from the ‘‘nested’’ relations as above. Function  $m_{VTP}$  could be defined by the optimized VTP mass, as calculated by the VTP supplier by the meso-level optimization problem:

$$\begin{aligned} m_{VTP} = & \min_{b_{VTP}} f_m(b_{VTP}, m_{rud}) \\ \text{bounded by:} & \underline{b}_{VTP} \leq b_{VTP} \leq \bar{b}_{VTP} \end{aligned} \quad (5)$$

Upper and lower bounds on the  $b_{VTP}$  are present. The rudder mass  $m_{rud}$  could be defined by the optimized rudder mass. This optimized mass is calculated by the rudder supplier by the local-level optimization problem:

$$m_{rud}(c_{rud}, F_{rud}, b_{rud}) = \min_{x_l} f_l(x_l, c_{rud}, F_{rud}, b_{rud}) \quad (6)$$

$$\begin{aligned} & \text{bounded by:} && x_l \leq x_l \leq \bar{x}_l \\ & \text{with} && b_{rud} = 0.90b_{VTP} \end{aligned} \quad (7)$$

Several local design variables  $x_l$ , e.g. skin thickness, number of ribs and hinges, could be considered.

The parameters  $c_{rud}, F_{rud}$  and  $b_{rud}$  are either constant parameters for the local objective function  $f_l$  or could be part of local constraint functions, depending on the implementation of the local rudder design and optimization tools.

The optimization problem formulation described above is based on a nested approach. The meso level (VTP) and local level (rudder) optimization is embedded in the global level optimization. The functions introduced depend on output from several analysis tools. These tools are introduced in the next subsection.

## B. Aircraft and Rudder design analysis tools

Within the AGILE project the design analysis is performed with several analysis tools provided by the AGILE partners. This analysis is carried out both on the aircraft and VTP level and on the rudder level. The tools that have been used for this particular study are:

- Overall Aircraft Design (OAD) analysis capability, provided by DLR as a remote service.
- Aeroelastic Modelling and Loads (AMLoad) analysis tool [5], provided by NLR.
- Hinge-System Design and Optimization Tool (HDOT) [6], provided by GKN Fokker for rudder MDO.
- High fidelity analysis of the rudder, see Section II.C, provided by CFS Engineering.

The procedure to evaluate a design using these tools is to first carry out an Overall Aircraft Design (OAD) analysis. The OAD analysis is a multidisciplinary analysis including full aircraft synthesis, tail plane resizing (e.g. following from the specified rudder mass), mass distribution and mission analysis. It produces aircraft design data in the Common Parametric Aircraft Configuration Schema (CPACS) format as used in AGILE, see [7].

Second, calculation of the loads on the rudder and the deflection of the rudder is carried out via AMLoad. AMLoad is an aeroelastic modelling and loads tool. The tool can perform loads calculation on both rigid as well as flexible structure. In this work the wings were assumed rigid. AMLoad can read the aircraft design data in CPACS format and extend it with loads analysis results.

Third, the rudder design is carried out via HDOT. HDOT performs a structural analysis of the rudder and carries out a design study where relevant objective and constraint functions can be chosen. In the present study, HDOT returns an

optimized rudder mass to the OAD analysis. Figure 3 depicts the workflow of the analysis tools, their interactions and the exchange of variables in the multi-level context. The remainder of this chapter further discusses the analysis tools that are applied to the design case.

In addition, an initial high fidelity analysis has been considered as well, see Section II.C.

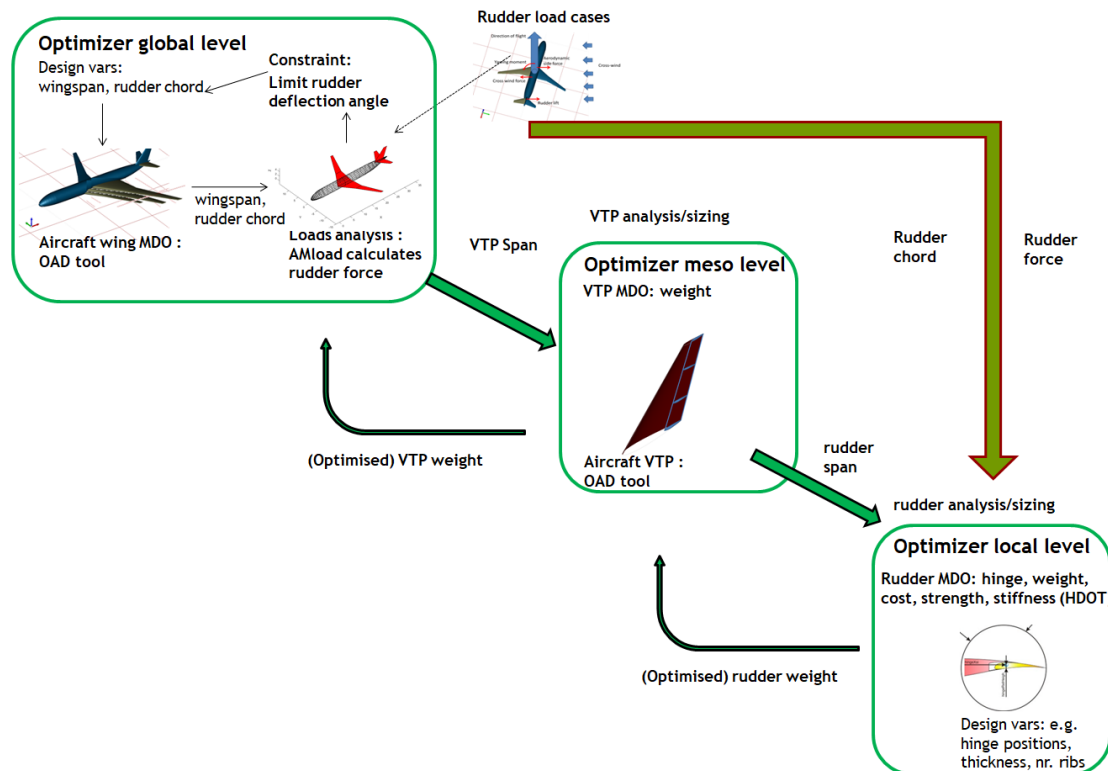


**Fig. 3** Workflow scheme of the aircraft rudder design tools in MLO context.

### 1. OAD analysis

The OAD analysis is composed by distributed design competences available at partner DLR of the AGILE project. These competences are targeted for conceptual and preliminary aircraft design activities. The competences included in the current study comprise both conceptual aircraft design methods [8] and physics based modules. Examples of the latter are aero-structural FEM based capabilities [9]. The OAD process is integrated as a fully automated multi-level workflow. In the global overall aircraft synthesis process the OAD process accounts for the input provided by the local level.

The OAD analysis is used for calculation of the global design objective. For the present study this global design objective is chosen as fuel mass and aircraft structural mass. An aircraft wing MDO with varying wing span has been chosen as global-level design case. However, the OAD tool can be used to carry out studies on other design parameters as well.

In addition to calculating overall aircraft properties, the OAD analysis tool has been used to identify a relation between VTP sizing and wing span sizing. Furthermore, a relationship between VTP sizing and rudder weight has been identified. These relations have been used to calculate VTP weight for changing wing span and rudder weights.

### 2. AMload

Aeroelastic Modelling and Loads (AMLoad)[5] is used for calculation of the loads on the rudder and the deflection of the rudder. The rudder deflection is used for calculation of the global constraint function. The rudder deflection may not exceed a certain maximum value. The rudder loads (represented by rudder force) are provided to the rudder level.

### 3. Hinge-System Design and Optimization

The Hinge-System Design and Optimization Tool (HDOT) [6] optimizes rudder hinge design with respect to rudder mass. As input the tool requires loads that are applied to the rudder hinges. Internally the tool carries out structural analysis to determine load paths and improve the size and position of the hinges. The tool is used at GKN Fokker and can be used for other type of design studies as well.

### 4. workflow

The workflow has an embedded hierarchy for which a formulation of a multi-level optimization can be derived. The OAD tool and AMLoad represent the global analysis tools, which are to be steered by a global optimizer. Minimizing the VTP mass corresponds to the meso level, here the VTP span and rudder mass are specified as parameter values. Finally, the HDOT represents the local level optimization. The rudder planform (here represented by rudder chord and rudder span for simplicity) and rudder force are specified as parameter values. They are fixed during the local optimization process itself. In Section III surrogate models are introduced to perform a nested optimization of the aircraft rudder design. These techniques support the final multi-level optimization formulation in Section IV.

## C. High fidelity analysis of the rudder

The analysis tools as described above are dedicated to conceptual or preliminary analysis of the rudder design. Later, in the design process (e.g. towards the detailed design) also high-fidelity analysis would be needed. The involvement of such tools may influence the results of the aircraft rudder MLO. In order to analyse and anticipate such impact a more detailed aerodynamic analysis of the rudder and the VTP is performed, using CFD. The CFD code of AGILE partner CFSE is applied.

The CFSE's solver NSMB (Navier-Stokes Multi-Block ) is a CFD solver using the cell-centered finite volume method on multi-block structured grids. The ANSYS® ICEM CFD™ pre-processor tool was used to generate the structured grid for the 3D aircraft configuration , and the chimera method was applied in order to simplify the mesh generation process, especially in the region of the rudder. The NSMB high-fidelity computation was performed using the 2<sup>nd</sup>-order Roe upwind space discretization scheme and the LU-SGS time integration scheme. Local time stepping was employed to accelerate the convergence to steady state. A fully turbulent flow was assumed, and the turbulence was modelled using the  $k - \omega$  Menter Shear Stress model.

AMLoad – as described above – calculates the rudder load, represented by the overall aerodynamic force acting on it. This calculation is based on an aerodynamic panel model which is less accurate for large control surface deflections. The panel method does not take into account three dimensional flow effects, such as flow separation, which may impact the overall force, especially in case of high rudder deflection angles. Initial calculations have been performed using the CSFE CFD code to visualize the three dimensional effects due to the rudder deflection, see Figure 4 and Figure 5. A flow analysis of one aircraft configuration has been performed, see Figure 4. This figure shows skin friction lines on the rudder. It shows that especially around the bottom of the rudder turbulence appears, which will impact the resulting overall aerodynamic force on the rudder. Further CFD analyses are part of ongoing work and could be detailed in a follow-on paper.

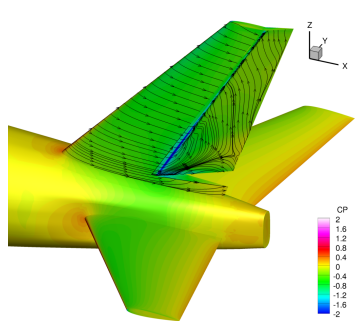


Fig. 4 Skin friction lines on the rudder explain the strong 3D effect of the flow on this part.

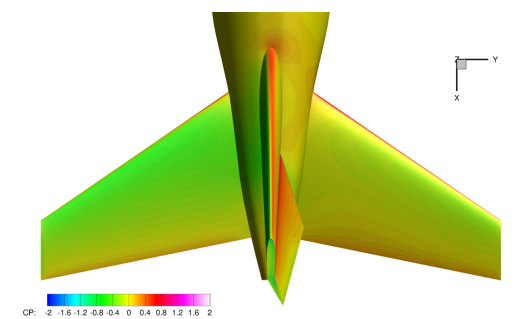


Fig. 5 The top view of the pressure coefficient close to the HTP/VTP region highlights also the effect of the rudder deflection on the pressure distribution on the HTP.

### III. Surrogate modelling and nested optimization

The present section introduces the surrogate models that are created to replace the more computationally expensive expert tools. A surrogate model is an analytical formula that replaces a complex model by means of data fitting, see e.g. [10] or [11]. Clearly, a surrogate model requires only small computation time. This is particularly useful in case a complex analysis (e.g. an analysis with HDOT) is applied multiple times as part of an optimization loop. In this study surrogate models are used to represent the analyses on aircraft level, vertical tail level and local rudder level. Finally, a nested optimization (Equation 4) is performed using the surrogate models.

#### A. Surrogate models derived from the analysis tools

A Design of Experiments (DoE) based on Latin Hypercube Sampling (LHS) has been created for analyzing 30 aircraft configurations with the OAD capability. In the parametric aircraft model the wing area is kept constant while varying wing span between 25 m and 30 m as well as the rudder root chord between 1.2 m and 1.7 m and the VTP mass between 300 kg and 380 kg. During the OAD simulations the aircraft mission is repeated for each analysis.

The OAD simulations provided a data set of 30 aircraft configurations. Analyzing this data set relations between several variables have been determined. The aircraft level mass variables Operating Empty Mass (OEM) and Maximum Fuel Mass (mFuelMax) can be predicted as a function of wing span and VTP mass. The VTP mass consists of the rudder mass and the fixed tail section mass. The mFuelMax corresponds to the maximum fuel mass needed for the mission. The prediction function was derived using a second order polynomial regression. The fit results are plotted in Figure 6. Points that are evaluated using the polynomials are plotted together with the fitting data set in Figure 6. The fitting data set covers the points that were computed for the DoE of 30 aircraft configurations. The polynomials have small prediction errors. The root mean squared error (RMSE) is less than 0.1% of the output data to be predicted, when evaluated on the fitting data set.

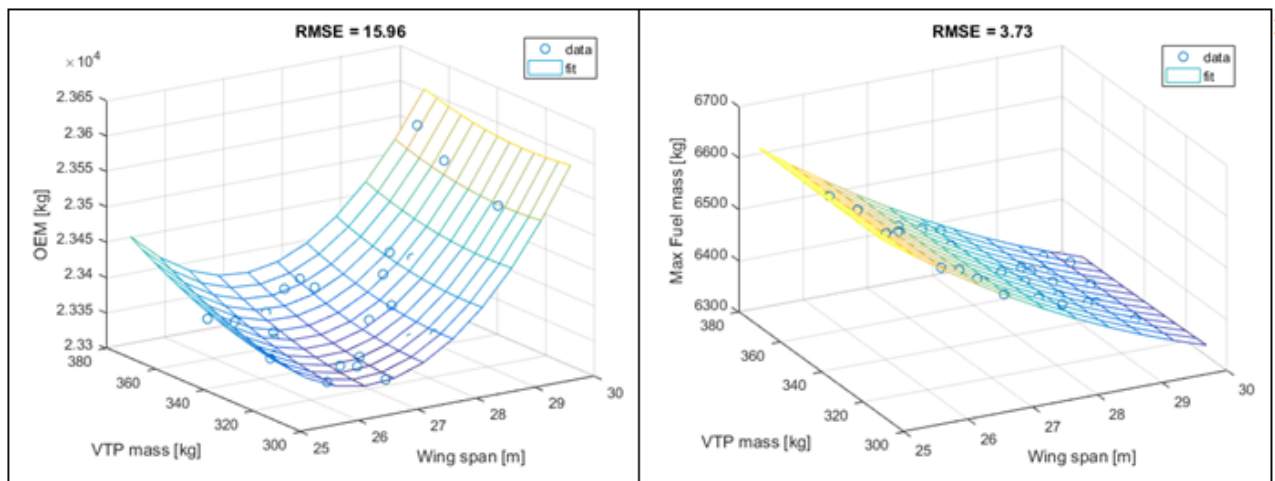


**Fig. 6** Surrogate model prediction of OEM (left) and max. fuel mass (right) derived from the OAD simulation data. In addition, the root mean squared error (RMSE) of the surrogate model prediction is displayed.

Figure 6 shows that for increasing wing span the OEM increases (more wing stiffeners are needed). The fuel mass decreases for increased wing span. This is due to increased efficiency of the wings during cruise (less induced drag). Therefore, less fuel is required to complete the mission that is simulated for the OAD analysis.

The OAD simulation data has been further processed by AMLoad in order to calculate the corresponding rudder loads and rudder deflection for each aircraft configuration. From the AMLoad results relations have been derived between the rudder root chord, the wing span and the rudder lateral force. In addition, relations have been identified between the rudder root chord, the wing span and the rudder deflection. These relations are shown in Figure 7. The latter relation is important for the optimization constraint that follows from the rudder load case: typically the rudder deflection has an upper limit to prevent flow separation. This means that if the deflection exceeds this limit a larger rudder, i.e. a larger rudder chord is needed.

The data was fitted via an interpolating kriging model with a 2<sup>nd</sup> order polynomial regression and Gaussian correlation function. The surrogate model is based on an interpolating function. The predicted points from this

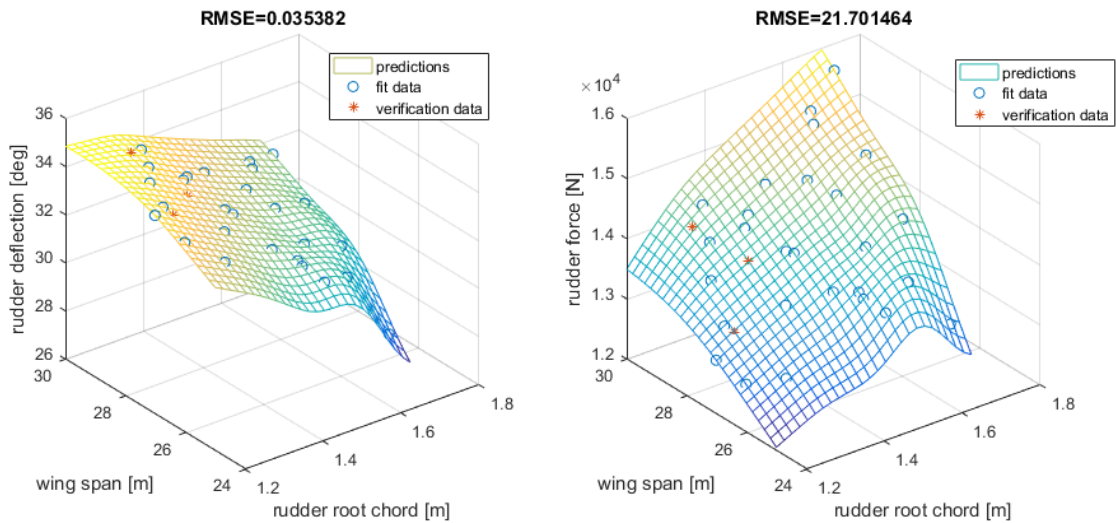


**Fig. 7** Surrogate model prediction of rudder deflection (left) and rudder load (right), derived from the AMLoad simulation data. In addition, the root mean squared error (RMSE) of the surrogate model prediction is given above the plot.

interpolating function have been verified by calculating the RMSE on three randomly chosen data points. These data points were excluded from the fitting data set (see the red stars in Figure 7). This results in an RMSE that is three orders of magnitude smaller than the actual data (i.e. the fitted outputs represented by the z-axes of 7).

Additional verification of the surrogate model was performed with the leave-one-out method. With this method one data point is excluded from the fitting set. This data point is reserved to verify the predicted point coming from the surrogate model. The excluded data point is then shifted over the complete data set, resulting in 30 fits (each time performed on the remainder of 29 data points) and 30 verifications. For each verification the deviation between the prediction and the actual output value in the excluded data point is calculated. From all 30 deviations one RMSE value is derived. The RMSE values are approximately 0.14 degrees for rudder deflection and 60 N for the rudder force prediction. Both RMSE values are approximately 0.5 % of the predicted output. The data fits and verification have been carried out using NLR's in-house MATLAB-based tool MultiFit [10].

On the VTP level the VTP mass can be predicted as function of the VTP span and rudder mass (following Equation 2). The OAD data set was used to derive this (linear) relation, see Figure 8. The prediction error is small. The RMSE is less than 0.01% of the data to be predicted.

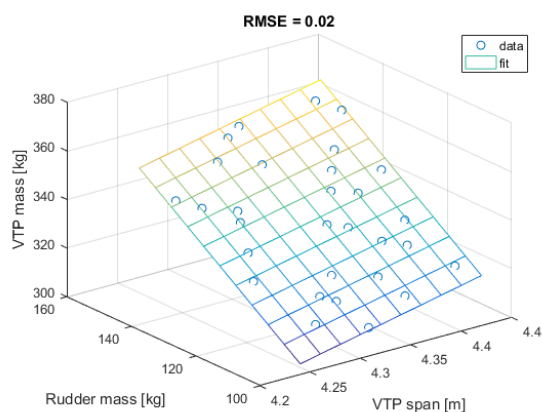


**Fig. 8** Surrogate model prediction of VTP mass derived from the OAD simulation data. In addition, the root mean squared error (RMSE) of the surrogate model prediction values are given above the plot.

In addition, to facilitate the couplings between the aircraft level and VTP level, and VTP level and rudder level, linear relations have been found in the OAD data set between VTP span and wing span (following Equation 1), and rudder span and VTP span. These relations are illustrated in Figure 9. The prediction errors – illustrated by the RMSE – are several orders of magnitude smaller than the data.

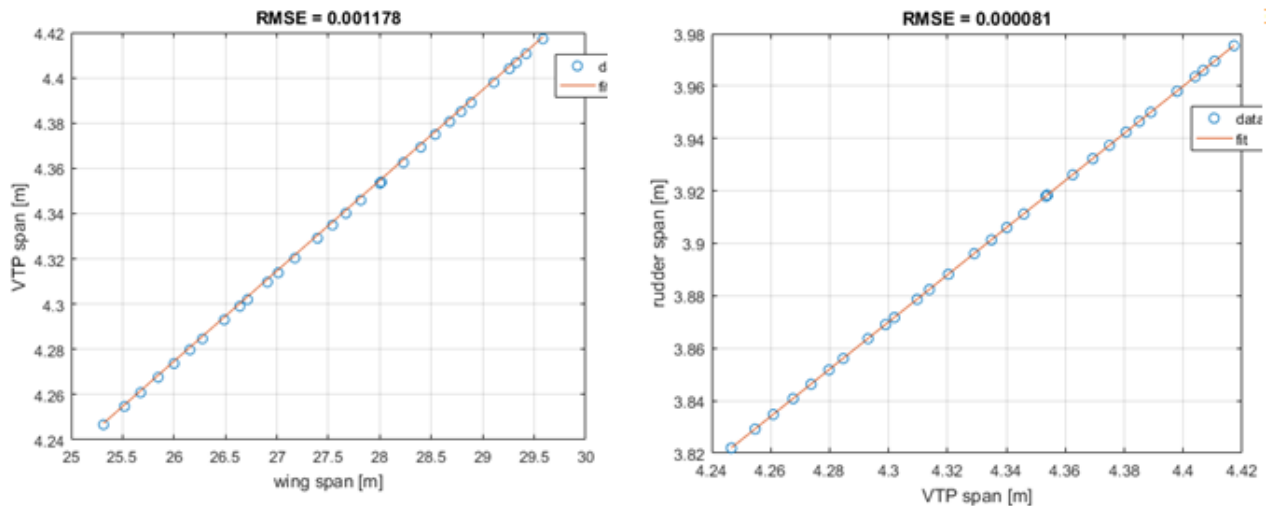


**Fig. 9** Surrogate model prediction of coupling variables VTP span (left) and rudder span(right) derived from the OAD simulation data. In addition, the root mean squared error (RMSE) of the surrogate model prediction is displayed.

On the rudder level, HDOT calculates the optimized mass of the rudder hinge assembly. Rudder loads (e.g. force) and rudder planform (e.g. chord) can be provided as parameter values. Figure 10 shows the relation between the optimized mass of the rudder hinge assembly and rudder lateral force. Note that non-linear effects appear due to step changes in the optimized design. These effects are caused by the use of discrete local variables (e.g. the number of parts or the chosen material) applied. Therefore, this relation is interpolated by piecewise polynomial functions.

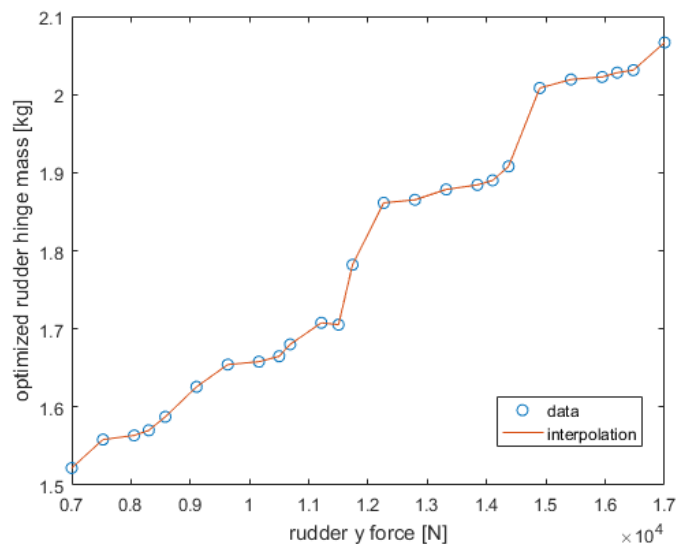


**Fig. 10** Surrogate model prediction of optimized rudder hinge mass, based on HDOT data.

Data of the full rudder mass were not available. Instead normalized data showing the effect of design changes was provided. Therefore, the HDOT results are scaled to the level of a rudder mass – between 100 and 150kg as applied in

the OAD analysis - , using the rudder chord, the rudder span and a additional scaling factor ( $\kappa_{sc}$ ):

$$m_{rud} = m_{\text{HDOT}} \cdot c_{rud} \cdot b_{rud} \cdot \kappa_{sc} \quad (8)$$

## B. Aircraft rudder optimization results with the surrogate models

As objective function a weighted sum of the aircraft Operating Empty Mass [kg] and the Maximum Fuel Mass ( $m_{\text{FuelMax}}$ ) [kg] is used, see Figure 6. Using  $\alpha_1$  and  $\alpha_2$  as the weight factors, the objective function is written as:

$$f_{obj} = \alpha_1 \cdot m_{\text{OEMass}} + \alpha_2 \cdot m_{m_{\text{FuelMax}}} \quad (9)$$

The compound objective function  $f_{obj} = f_{obj}(c_{rud}, b)$  is calculated by performing the following steps:

- Calculate the VTP span  $b_{VTP}$  based on the wing span  $b_{wing}$ .
- Calculate the rudder force as function of rudder root chord  $c_{rud}$  and the wing span  $b_{wing}$ , using the AMLoad derived surrogate model, see Figure 7.
- Calculate the (locally) optimized rudder mass as function of the rudder force, the rudder root chord and the rudder span  $b_{rud} = 0.9b_{VTP}$ , using the HDOT derived surrogate model, see Figure 10.
- Calculate the VTP mass as function of VTP span and rudder mass  $m_{rud}$ .
- Calculate the aircraft Operation Empty Mass and Maximum Fuel Mass as function of wing span and VTP mass, using the OAD derived surrogate model, see Figure 6.
- Calculate the weighted sum, see Equation 9.

As a constraint, a maximum rudder deflection of  $\theta = 32$  degrees is applied. The limit value here is used as an illustrative value. In practice, the rudder maximum deflection is lower because of aerodynamic and system limitations. The present limit is set higher to allow for more design freedom. For the rudder design problem setting a constraint on the rudder deflection reduces the possible rudder configurations. Without the maximum rudder deflection constraint some designs result in larger rudder deflection, this can be seen in Figure 7. The deflection is calculated as function of rudder root chord  $c_{rud}$  and wing span  $b_{wing}$  by using the AMLoad derived surrogate model (see Figure 7).

The optimization problem formulation that was introduced in the previous section in Equation 4 is now filled in as follows:

$$\begin{aligned} \min_{b_{wing}, c_{rud}} f_{obj} = & \alpha_1 * m_{\text{OEMass}}(b_{wing}, m_{\text{VTP}}(c_{rud}, b_{wing})) + \dots \\ & \alpha_2 * m_{m_{\text{FuelMax}}}(b_{wing}, m_{\text{VTP}}(c_{rud}, b_{wing})) \quad (10) \\ \text{subject to:} & \theta_{rud}(b_{wing}, c_{rud}) \leq 32 \\ \text{bounded by:} & \underline{b}_{wing}, \underline{c}_{rud} \leq b_{wing}, c_{rud} \leq \bar{b}_{wing}, \bar{c}_{rud} \end{aligned}$$

The optimization has been performed in MATLAB using a sequential quadratic programming (SQP) method [12]. The necessary optimization iterations are shown in Figure 11. Different weight factors ( $\alpha_1, \alpha_2$ ) have been applied to assess the sensitivity of the optimized design. A larger value of  $\alpha_1$  results in a lower OEMass and in a larger fuel mass.

Table 1 shows the SQP optimization results with varying values of the weight factors  $\alpha_1$  and  $\alpha_2$ . The optimized design varies from a large wing span with a low fuel mass and a relatively high VTP mass, to a small wing span with a higher fuel mass and lower VTP mass.

Weight values	rudder root chord [m]	wing span [m]	VTP mass [kg]	rud mass [kg]	OEM mass $m_{\text{OEMass}}$	MaxFuelMass $m_{\text{FuelMax}}$
$\alpha_1, \alpha_2$						
1,0	1.4142	26.4935	320.3352	110.9455	2.3331e+04	0.65e+04
1,1	1.5249	27.8536	337.1677	122.9225	2.3370e+04	0.6427e+04
0,1	1.7	29.7465	368.8178	147.8126	2.3568e+04	0.6328e+04

**Table 1** SQP optima, with varying values of the weight factors  $\alpha_1$  and  $\alpha_2$ .

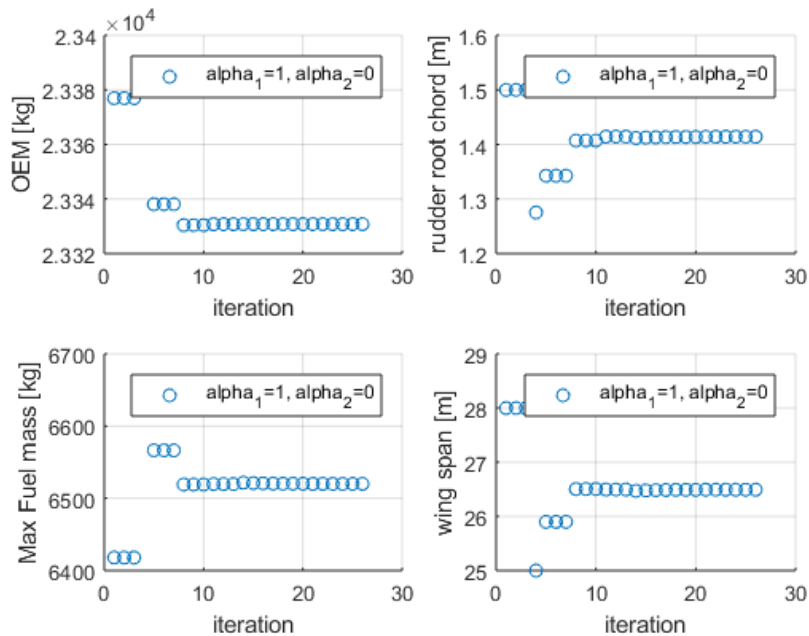


**Fig. 11 Results of the nested optimization approach. Optimization iterations with objectives (left) and design parameters (right) and  $\alpha_1 = 1$ . Hence, minimum of  $m_{\text{OEMMass}}$ .**

In case the wing span increases, the rudder root chord increases as well. This effect is enforced by the optimization constraint function: a large wing span increases both the rudder force and deflection. If the deflection exceeds the deflection limit, the rudder chord needs to be enlarged, in order to enable the yaw moment compensation with a smaller rudder deflection.

The OAD tool has the possibility to plot the designs that have been evaluated by the tool. Therefore, the results of the three optimized designs together with a reference design are shown in Figure 12 and Figure 13. The reference aircraft configuration in this case has a wing span of 27.18 [m] and a rudder root chord of 1.4651 [m].

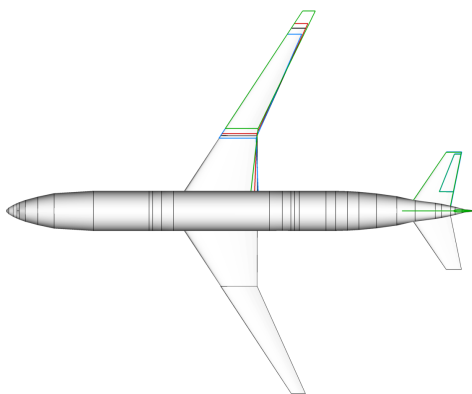


**Fig. 12 Wing planform comparisons of optimal designs: 1-blue, 2-red, 3-green (with increasing wing span) versus the baseline configuration (black).**

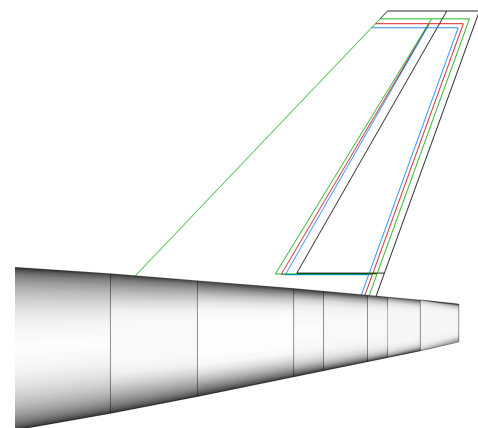


**Fig. 13 Vertical Tail Plane comparisons of optimal designs: 1-blue, 2-red, 3-green (with increasing wing span) versus the baseline configuration (black).**

#### IV. MLO process via concept of Analytical Target Cascading (ATC)

Various approaches can be followed to deal with the aircraft rudder MLO use case. In the past decades, many methodologies have been investigated for MLO approaches in engineering problems. For example, overviews can be found in the PhD dissertation of De Wit [13], the overview of Balling and Sobieski [14] and the survey of Martins and Lambe [15]. In the present work the approach followed in [3] is used where an additional meso level is added to the problem formulation. Furthermore, coupling constraints are now embedded between global, meso and local level as will be shown in the current section.

In essence, an MLO problem consists of a hierarchy of individual but coupled optimization problems. In contrast, in traditional (single-level) optimization the hierarchical (multi-level) nature of the underlying design problem is not explicitly accounted for in the optimization problem formulation.

MLO approaches typically consist of four sequential steps, see [13]. First, a hierarchy is identified in the considered system and/or design problem. Second, a decomposition (splitting) technique has to be defined based on the coupling characteristics. Third, a coordination strategy is defined. This involves setting up a procedure (i.e. define the rules) for communication between the decomposed but coupled subproblems. Finally, a job scheduling procedure is defined to have the sub problems communicate in the right sequence and corresponding to the computer architecture (e.g. sequential, parallel, or distributed).

A hierarchy can be naturally present in the process flow, e.g. along disciplines, departments or subcontractors that are involved in the design process. A hierarchy may also be introduced via e.g. a problem matrix [16] (also known as Functional Dependence Table [17]). In the present study of the aircraft rudder MLO use case the hierarchy is identified along the current process flow, in accordance with the hierarchy of the considered systems. An airframer designs an overall aircraft and subcontracts the VTP design. In its turn the VTP designer subcontracts the rudder design. At (global) aircraft level design variables are set, e.g. wing span. At meso level VTP design variables are set, e.g. for the VTP based on control specifications, manufacturing costs, available material. At the local level the rudder design variables are set, e.g. based on planform specifications, applied forces, manufacturing costs and available manufacturing material. Figure 14 shows an abstract representation of the levels present in the current design case.

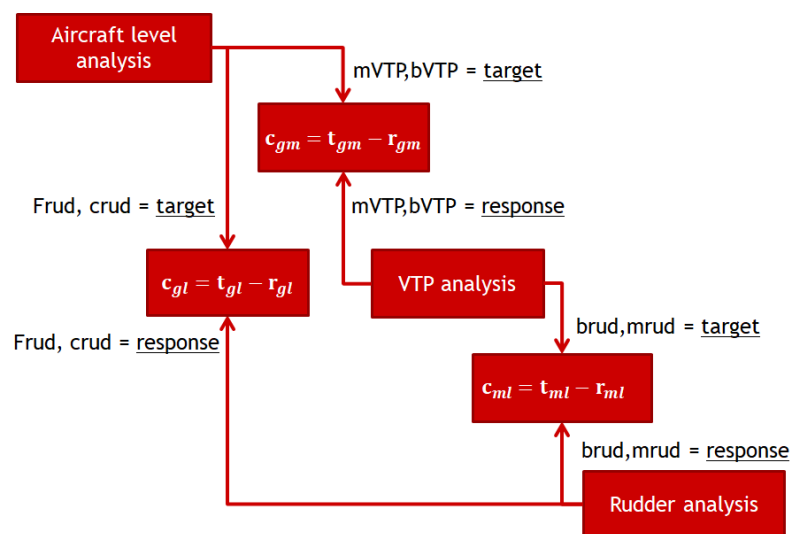


**Fig. 14** Introducing consistency constraints according to the ATC approach in a coupled MLO problem.

In Figure 14 the global level calculations are carried out with an “expected” VTP mass and rudder chord. Furthermore, forces applied to the rudder are calculated at global level and the VTP span is calculated at global level. These four values are so-called “target” values ( $T$ ), i.e. these values have to be met at the meso and local level. These “target” values are sent to the meso and local level. At meso and local level computations are carried out to meet the “target” values. Because the targets are rigid in Figure 14, the meso and local level have the option of communicating back “responses” ( $R$ ) that are in agreement with the targets; i.e. “come up with a VTP and rudder design that fulfills the expectations at global level and meets all requirements at meso and local level”. In case all requirements for the targets that have been set cannot be met at meso and local level, an inconsistency is measured between targets and responses.

The inconsistency is measured with the consistency ( $C_{gm}$  and  $C_{gl}$ ) constraint functions.

Likewise, between meso level and local level calculations are carried out with an “expected” rudder mass. Furthermore, the rudder span is calculated at meso level. These “target” values are send from meso to local level. At local level computations are carried out to meet the “target” values. Hence, at local level a rudder is designed that fulfills both the targets from the global level as well as the meso level. In case the requirements cannot be met the inconsistency is measured with the constraint function  $C_{ml}$ .

The consistency constraints can be evaluated on the global level, meso level and the local level, or at each level. In our case the consistency constraints are evaluated at each level. Therefore, each target variable has a “copy” at the lower level and each response variable has a “copy” at the higher level. Figure 15 depicts the decomposed optimization problem with the consistency constraints (on global, meso and local level).

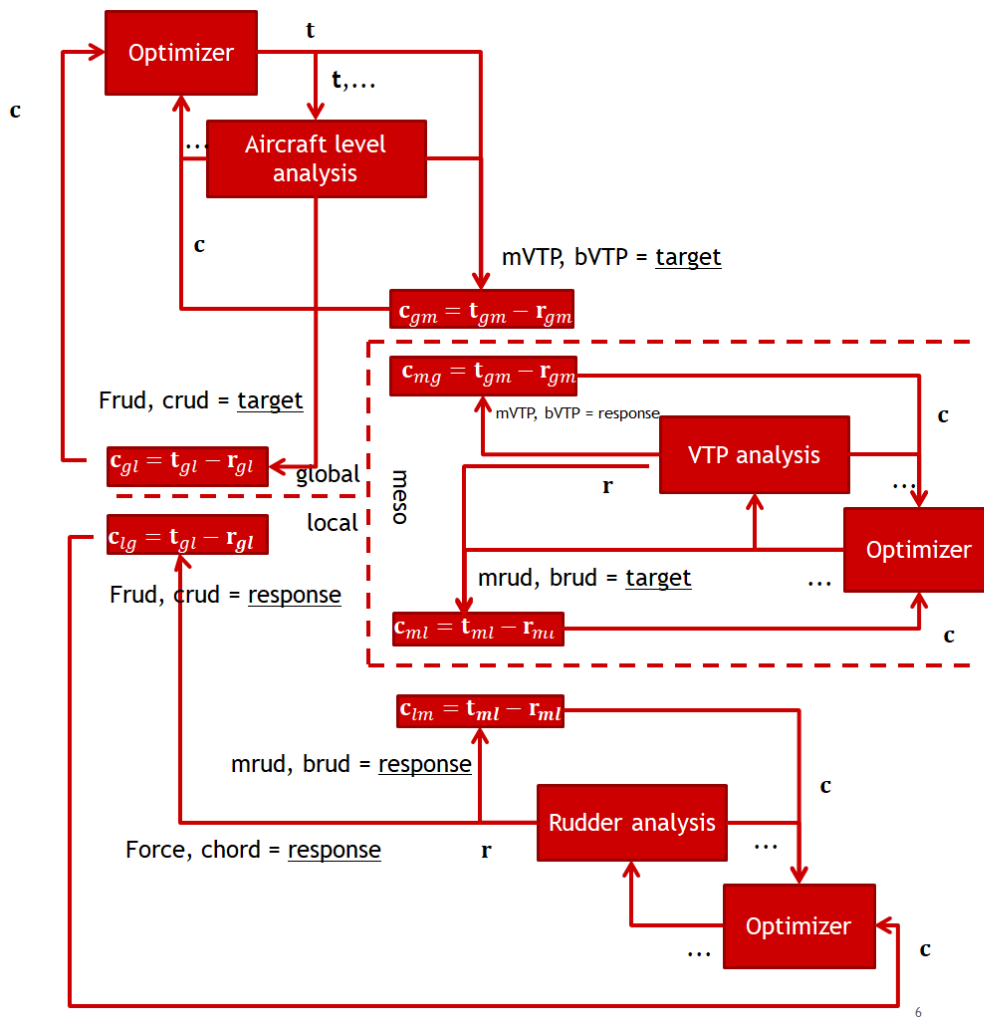


Fig. 15 Decoupled aircraft, VTP level and rudder level optimization in ATC based MLO.

Once consistency constraints have been formulated they are decomposed via a strong (equal) or weak (relaxed) formulation [18]. Both choices have their advantage or disadvantage. A strong formulation usually involves computing sensitivity of the individual optimization problems with respect to changes to the coupling or adding variables to calculate how the individual optimization problem reacts on external changes (changes due to the coupling). A weak formulation involves an additional approach to relax the consistency constraints e.g. by a penalty as function of the constraint deviations. In the present paper a choice was made to relax the consistency constraints to avoid additional programming steps that are necessary to implement a strong (equal) formulation.

To apply the technique of ATC the consistency constraints are relaxed via a so-called Augmented Lagrangian Penalty function [4]. This function is expressed as a function of the consistency:  $\pi(C)$ . The relaxed consistency constraints are

then mathematically expressed as:

$$\pi(\mathbf{C}) = \mathbf{v}^T \mathbf{C} + \|\mathbf{w} \circ \mathbf{C}\|_2^2. \quad (11)$$

The  $\circ$  symbol is used to denote a term-by-term multiplication of vectors. Two additional parameters are applied to derive a penalty function of the consistency violations (inconsistencies): the Lagrange multipliers  $\mathbf{v}$  and the penalty parameters  $\mathbf{w}$ . To determine values for these parameters a coordination strategy is necessary that is explained hereafter.

Initial values for the penalty parameters are set based on user experience. Alternatively, initial values can be calculated by evaluating the initial gap in consistency ( $\mathbf{C} \neq \mathbf{0}$ ). This can be accomplished by running each optimization problem using a very small penalty parameter. Each optimization problem in the hierarchy will then search for an optimal solution without considering the consistency with other problems in the hierarchy. This is explained in the work of Tosserams *et al.* [19]. In the present work an initial guess for each penalty parameter is used.

To achieve convergence of the relaxed global-local problem, the Lagrange multipliers are updated via:

$$\mathbf{v}^{k+1} = \mathbf{v}^k + 2\mathbf{w}^k \circ \mathbf{w}^k \circ \mathbf{C}^k \quad (12)$$

and the penalty parameters by:

$$\mathbf{w}^{k+1} = \beta \mathbf{w}^k \quad (13)$$

where  $\beta \geq 1$ , typically chosen between 2 and 3, see [4]. The  $k$  stands for the iteration number of updating the penalty parameters. These parameters are updated until the change in objective function values ( $f_{..}$ ) of global, meso and local level have become sufficiently small. Sufficiently small is in this case expressed by threshold  $\tau_{ATC}$  that is computed via:

$$\left\| (f_g + f_m + f_l)^k - (f_g + f_m + f_l)^{k-1} \right\|_{inf} \leq \tau_{ATC} \quad (14)$$

The entire optimization process (covering global, meso and local) is finished when in addition to the change in objective function values (Equation 14) the change in consistency has become sufficiently small. This is mathematically expressed as:

$$\left\| \mathbf{C}_{..}^k - \mathbf{C}_{..}^{k-1} \right\|_{inf} \leq \tau \quad (15)$$

Typically[4],  $\tau_{ATC}$  is chosen as:

$$\tau_{ATC} = \frac{\tau}{10}. \quad (16)$$

Finally, a job scheduling procedure is defined. Here, a sequential solution process is chosen. First the global optimization problem is solved (with initial response values). Second, the targets from the global system are communicated to the meso system and the meso system is optimized. Following the meso optimization the targets from meso system and global system are communicated to the local system, see the inner loops of Figure 16.

Third, a check for updating the Lagrange multipliers and penalty parameters is done, see the outer loop of Figure 16. The responses from local level are communicated to the meso and global system. Likewise the responses from meso level are communicated to the global system. This procedure is then repeated until the change in (in)consistencies  $\mathbf{C}$  has become sufficiently small, see Equation 15.

Applying the ATC approach (as described above) to the rudder optimization problem that was mathematically expressed in Equation 4 one obtains the following problem decomposition.

The global optimization problem is expressed as:

$$\min_{b_{wing}, \mathbf{T}_{gl}, \mathbf{T}_{gm}} f_g(b_{wing}, \mathbf{T}_{gl}) + \pi(\mathbf{C}_{gm}, \mathbf{C}_{gl}) \quad (17)$$

$$\text{subjected to:} \quad g(b_{wing}, \mathbf{T}_{gl}) \leq \mathbf{0} \quad (18)$$

$$\text{bounded by:} \quad \underline{b}_{wing}, \underline{\mathbf{T}}_{gl}, \underline{\mathbf{T}}_{gm} \leq b_{wing}, \mathbf{T}_{gl}, \mathbf{T}_{gm} \leq \bar{b}_{wing}, \bar{\mathbf{T}}_{gl}, \bar{\mathbf{T}}_{gm} \quad (19)$$

The meso optimization problem is expressed as:

$$\min_{\mathbf{R}_{gm}, \mathbf{T}_{ml}} f_m(\mathbf{R}_{gm}, \mathbf{T}_{ml}) + \pi(\mathbf{C}_{gm}, \mathbf{C}_{ml})$$

$$\text{bounded by:} \quad \underline{\mathbf{R}}_{gm}, \underline{\mathbf{T}}_{ml} \leq \mathbf{R}_{gm}, \mathbf{T}_{ml} \leq \bar{\mathbf{R}}_{gm}, \bar{\mathbf{T}}_{ml}$$

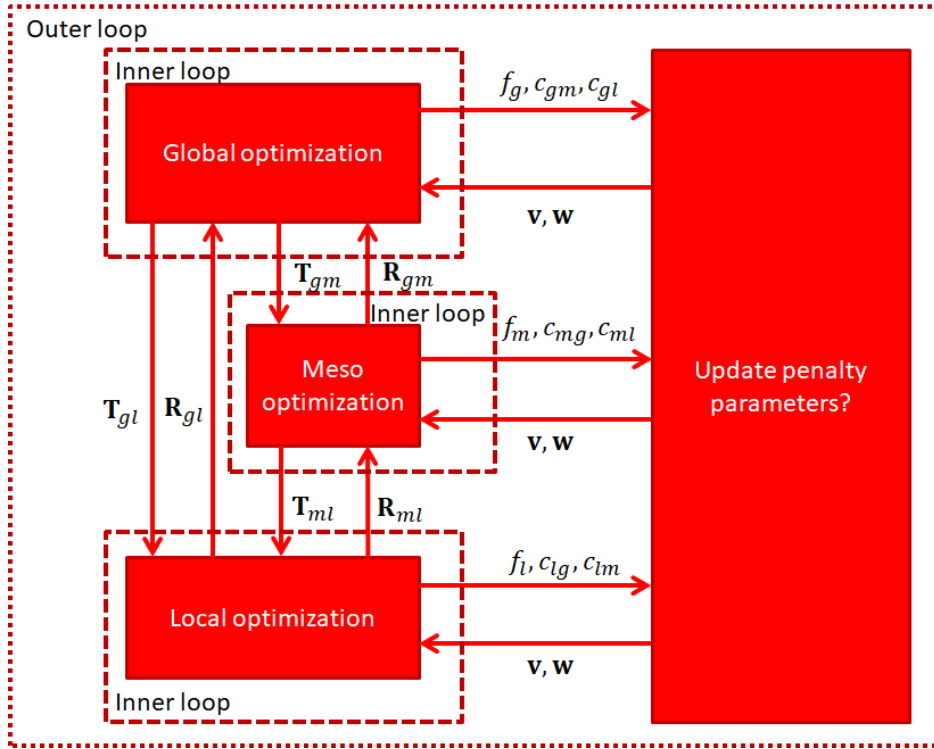


**Fig. 16** Sequential update process of the (sub)systems optimizations.

The local optimization problem is expressed as:

$$\min_{\mathbf{R}_{gl}, \mathbf{R}_{ml}} \quad f_l(\mathbf{R}_{gl}, \mathbf{R}_{ml}) + \pi(\mathbf{C}_{gl}, \mathbf{C}_{ml})$$

bounded by:  $\underline{\mathbf{R}}_{gl}, \underline{\mathbf{R}}_{ml} \leq \mathbf{R}_{gl}, \mathbf{R}_{ml} \leq \overline{\mathbf{R}}_{gl}, \overline{\mathbf{R}}_{ml}$

With  $b_{wing}$  the wing span,  $\mathbf{T}_{gl}$  the target values of the coupling variables (rudder chord  $c_{rud}$  and rudder force  $F_{rud}$ ),  $\mathbf{T}_{gm}$  the target value of VTP mass  $m_{VTP}$ ,  $\mathbf{R}_{gm}$  the (meso level) response of the coupling variable (VTP mass  $m_{VTP}$ ). The target values  $\mathbf{T}_{ml}$  of the coupling variables ( $b_{rud}$ ,  $m_{rud}$ ) and  $\mathbf{R}_{ml}$  the (meso level) responses of the coupling variables (thus, rudder span  $b_{rud}$ , rudder mass  $m_{rud}$ ). Furthermore,  $\mathbf{C}_{gm}$ ,  $\mathbf{C}_{gl}$  and  $\mathbf{C}_{ml}$  the consistencies on global, meso and local level.  $\pi$  is the penalty function as described above and  $f_g$ ,  $f_m$  and  $f_l$  are the global, meso and local objective functions.

The functions  $f_g$ ,  $f_m$  and  $f_l$  have been previously introduced. Using the target and response variables these equations are mathematically expressed via:

$$\begin{aligned} f_g(c_{rud}, b_{wing}) &= & f_{obj} &= \alpha_1 * m_{OEMass} + \alpha_2 * m_{MaxFuelm} \\ g(c_{rud}, b_{wing}) &= & & \theta - 32 \leq 0 \\ f_m(b_{wing}, m_{rud}) &= & & m_{VTP} \\ f_l(c_{rud}, F_{rud}) &= & & m_{rudder} \end{aligned} \quad (20)$$

Furthermore, a rudder force calculation is used:  $F_{rud} = f_{AML}$ , rudder (scaled) mass:  $m_{rud} = f_l(c_{rud}, F_{rud}, b_{rud})$  a VTP mass:  $m_{VTP} = f_{mVTP}(b_{VTP}, m_{rud})$ . The rudder mass is scaled because the exact mass output of the rudder was not available, see subsection III.A.

The global, meso and local optimization problems have been implemented in MATLAB and solved via the ATC procedure. The global, meso and local optimizations have been performed with a sequential quadratic programming (SQP) method, using finite difference approximation of the derivatives. The iteration history of the coupling variables during the ATC process are shown in Figure 17, Figure 18, Figure 19 and Figure 20.

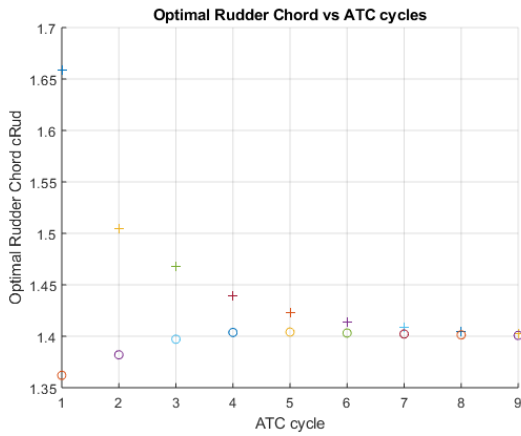


**Fig. 17** Iteration history of the ATC algorithm. Values of computed rudder chord versus number of ATC cycles. The "+" symbols represent values calculated at global level. The "o" symbols represent values calculated at local level.

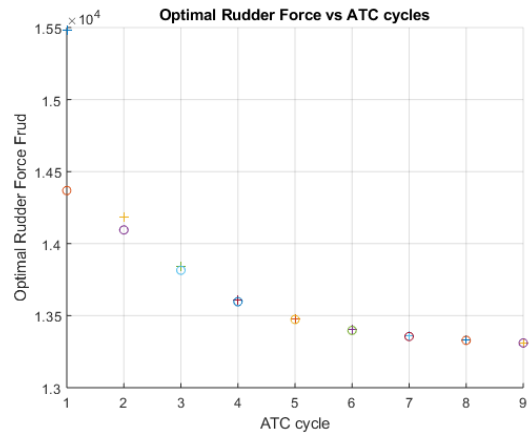


**Fig. 18** Iteration history of the ATC algorithm. Values of computed rudder force versus number of ATC cycles. The "+" symbols represent values calculated at global level. The "o" symbols represent values calculated at local level.

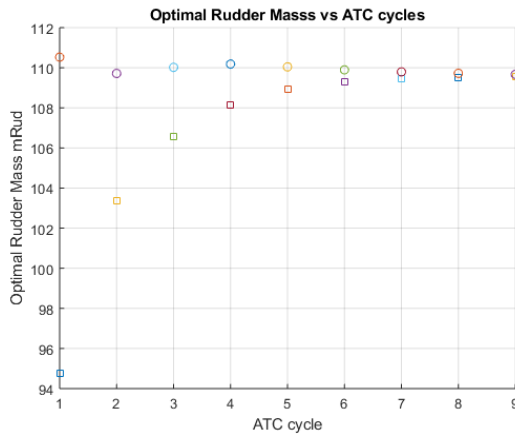


**Fig. 19** Iteration history of the ATC algorithm. Values of computed rudder mass versus number of ATC cycles. The "□" symbols represent values calculated at meso level. The "o" symbols represent values calculated at local level.

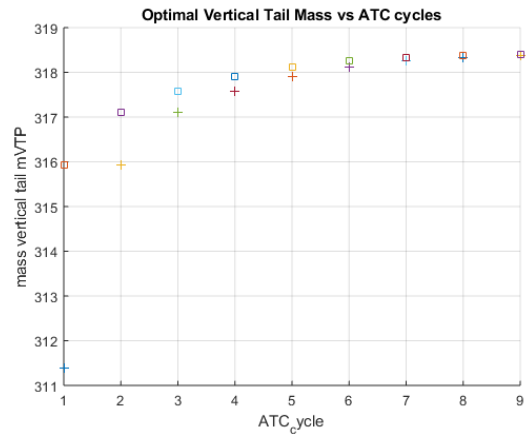


**Fig. 20** Iteration history of the ATC algorithm. VTP mass versus ATC cycles. The "□" symbols represent values calculated at meso level. The "+" symbols represent values calculated at global level.

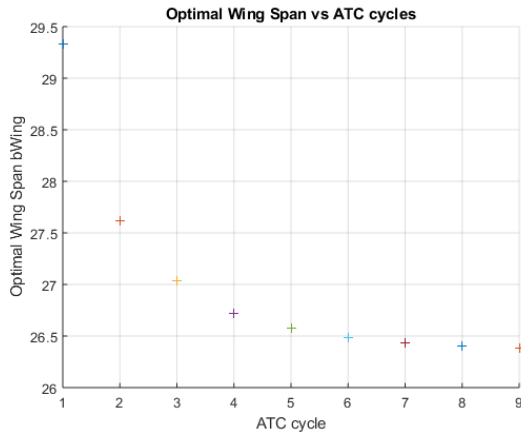


**Fig. 21** Wing Span versus ATC.

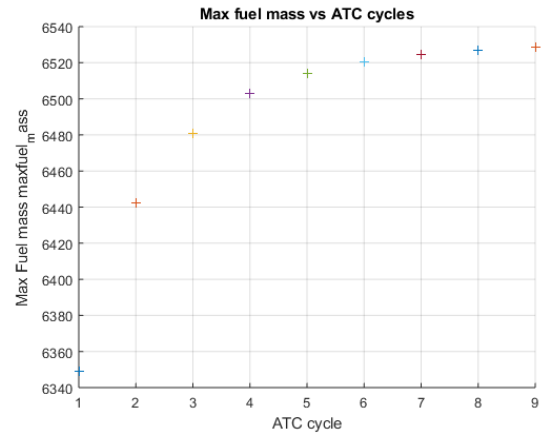


**Fig. 22** Max Fuel Mass versus ATC cycles.

The iteration history of the outer loop is reflected in figures 17, 18, 19 and in Figure 20 for the global value VTP mass ( $m_{VTP}$ ). These figures show the history of global, meso and local optimal rudder chord  $c_{rud}$ , rudder force  $F_{rud}$  and rudder mass  $m_{rud}$ . The initial differences between the targets (in the figures denoted "+") and responses (in the figures denoted "o" for local and "□" for meso) are relatively large. Hence, when left to itself the global optimum value for VTP weight and fuel mass corresponds to a rudder chord, rudder force and rudder mass that is different from the optimum rudder weight.

The augmented Lagrangian penalty function pushes the global and local level objective and constraint functions to move the target values and response values closer to an agreement (consistency). After 9 cycles of inner and outer loop, consistency is within acceptable tolerance ( $\tau \leq 0.01$ ) and a corresponding optimum solution for global and local objective function has been found. This global and local optimum is feasible for both global and local optimization problem. Compared to the nested optimization (see Figure 11) this results in a smaller number of data exchanges between global and local level.

The iteration history of the inner loop is reflected in Figure 21 for global design variable wing span  $b$  and in Figure 22 for global value max fuel mass ( $m_{MaxFuel}$ ).

The ATC parameters were tuned to get a consistent solution between global and local optimization as quickly as possible starting from an arbitrary feasible design. Parameters that can be tuned are the initial penalty parameters  $\nu^k$ , the consistency tolerance  $\tau$  and penalty update parameter  $\beta$ . In the present setting, initial penalty parameters were set to  $\nu^k = 10$ , the consistency tolerance to  $\tau = 0.005$  and penalty update parameter to  $\beta = 3$ .

In case the initial value of  $\nu^k$  is high, the global and local optimization problem have little room to adjust the target or response value to a value other than the initial one. Hence, little design freedom is given to reach consistency. The consistency tolerance  $\tau$  is a measure how well the target and response at the interface between global and local meet. A loose setting (high  $\tau$ ) may cause premature convergence of global and local level arriving at a non-optimal overall design. Likewise, a tight (low  $\tau$ ) setting may cause endless exchange of targets and responses between global and local level while the overall design doesn't change. The penalty update parameter  $\beta$  is a setting to scale the penalty parameters. The higher the value of  $\beta$ , the faster global and local target and response values meet. Hence, less design freedom is given to the individual optimization problems. Contrary, the lower this value, the more design freedom is given at the expense of more exchange of target and response values between the global and the local level.

The iteration history shown in Figures 21, 20 and 22 converges to the optimum that was found with the nested approach. By changing weight factors ( $\alpha_1$  and  $\alpha_2$ ) in the MLO formulation the optima that were found with the nested approach are reproduced. This is shown in Table 2.

Weight values	rudder root	wing span	VTP mass	rud mass	OEM mass	MaxFuelMass	ATC
$\alpha_1, \alpha_2$	chord [m]	[m]	[kg]	[kg]	$m_{OEMass}$	$m_{FuelMax}$	iterations
1,0	1.4142	26.4941	320.3314	110.9435	2.3331e+04	6.5200e+03	9
1,1	1.5142	27.3926	333.1231	120.5245	2.3349e+04	6.4564e+03	14
0,1	1.7	29.7465	356.8273	141.3449	2.3555e+04	6.3275e+03	14

**Table 2 ATC MLO optimization results for different  $\alpha_1$  and  $\alpha_2$**

In Table 2 the results are listed for various weights ( $\alpha_1$  and  $\alpha_2$ ) settings in the objective function  $f_{obj}$  to reproduce the optima found with the nested optimization approach. The ATC settings were set at default settings with initial ( $k=1$ ) penalty weight  $\nu^1 = 10$ , consistency setting  $\tau_{atc} \leq 5e - 3$  and  $\beta = 3$ .

For ATC to work efficiently, all design variables and optimization functions need to be scaled to unity. The designs that are found are in good agreement with the nested approach. The small differences are due to small inconsistencies. In case the  $\tau_{atc}$  is set very low the number of ATC iterations increases but the optimum found better corresponds to the nested optimum found. As a result, a balance between performance and inconsistency setting was found that was considered sufficient.

From this MLO exercise it can be seen that individual optimizations on each level may provide conflicting design results. A strategy, such as ATC provides a common understanding of the design problem, establishes interfaces in the design problem and integrates both optimizations and synchronizes the results, taking into account the mutual inter-dependencies. Due to the division in inner and outer loops the number of exchanges between global and local level is smaller than if a nested approach would be applied thereby reducing the risk of late design changes.

The current MLO case could be further extended with additional disciplines. E.g. sizing of the wing planform as a

second discipline where aerodynamic considerations are taken into account below the global OAD computations. In this context HDOT could be applied as well to contribute to the design of the wing moveables. Furthermore, a power plant discipline could be added to analyze fuel flow as a function of thrust requirement due to wing and VTP sizing in the neighboring disciplines.

## V. Conclusions

A multi-level optimization approach to a coupled aircraft rudder design problem has been presented. An MLO method based on Analytical Target Cascading is used for decoupling the optimization problem into an aircraft (global) level optimization problem, a vertical tail (meso) level and rudder (local) level optimization problem. Each problem is solved separately, while enforcing the couplings by consistency constraints. The level of consistency is checked after each global, meso and local optimization in an iterative process. As a starting point (reference) the same problem has been solved using a nested optimization approach as well. The ATC method and nested optimization method arrive at the same design optima. However, in the case of ATC the number of communication events between the global and the local level becomes smaller than with the nested approach, in which the meso and local optimization is part of the global objective function. Limiting the amount of interaction is needed in order to create an efficient collaboration between the aircraft OEM (performing the global optimization) and the suppliers (performing the meso and local optimizations). Furthermore, in setting up the MLO problem OEM and suppliers obtain a common understanding of the design problem. Together interfaces are established in the design process and thereby the risk of late changes is reduced.

The aircraft rudder MLO use case is illustrated by applying surrogate models that were derived from aircraft and rudder design analysis competences available from the AGILE project. The surrogate models provide an efficient approach for running the MLO.

Using MLO the OEM and supplier are able to significantly reduce the development time of an aircraft (sub)system. Automation and a common understanding of the communication reduces the chance of miscommunications and corresponding rework. In addition, the surrogate models that are part of MLO could be used to shield the intellectual property (IP) of both OEM and supplier and could provide flexibility when performing conceptual design. This would allow for a better collaboration in situations where contracts have not been signed and IP issues can be sensitive.

In a next step, more disciplines could be added to the analysis and optimization. For example, sizing of the wing planform involving an aerodynamic discipline could be added and/or a power plant discipline to demonstrate the interaction between disciplines in the design process. The MLO approach can be easily extended to much larger and more complex hierarchies.

## Funding Sources

The research presented in this paper has been performed in the framework of the AGILE project (Aircraft 3rd Generation MDO for Innovative Collaboration of Heterogeneous Teams of Experts) and has received funding from the European Union Horizon 2020 Programme (H2020-MG-2014-2015) under grant agreement no. 636202.

The Swiss participation in the AGILE project was supported by the Swiss State Secretariat for Education, Research and Innovation (SERI) under contract number 15.0162.

## Acknowledgments

The authors are grateful to the partners of the AGILE Consortium for their contribution and feedback.

## References

- [1] EASA, “Certification Specifications and Acceptable Means of Compliance for Large Aeroplanes CS-25, section CS 25.147 Directional and lateral control,” , 2018. URL <http://www.easa.europa.eu>.
- [2] Lammen, W., de Wit, B., Vankan, J., Timmermans, H., van der Laan, T., and Ciampa, P., “Collaborative Design of Aircraft Systems - Multi-Level Optimization of an Aircraft Rudder,” *Aerospace Europe 6th CEAS Conference*, CEAS Council of European Aerospace Societies, 2017.
- [3] de Wit, A., Lammen, W., Vankan, W., Timmermans, H., van der Laan, T., and Ciampa, P., “Aircraft rudder optimization - a multi-level and knowledge-enabled approach,” *Progress in Aerospace Sciences*, Vol. accepted - to be published, 2018.
- [4] Tosserams, S., Etman, L., Papalambros, P., and Rooda, J., “An augmented lagrangian relaxation for analytical target cascading,” *Structural and Multidisciplinary Optimization*, Vol. 31, 2006, pp. 176–189.
- [5] Timmermans, H., and Prananta, B., “Aeroelastic challenges in the Aircraft Design Process,” *READ and SCAD conference*, 2016.
- [6] Kulkarni, A., van Dijk, R., van den Berg, T., and Rocca, G. L., “A knowledge based engineering tool to support front-loading and multi-disciplinary design optimization of the fin-rudder interface,” *Aerospace Europe 6th CEAS Conference*, ????
- [7] van Gent, I., Aigner, B., Beijer, B., Jepsen, J., and Rocca, G. L., “Knowledge architecture supporting the next generation of MDO in the Agile paradigm,” *PIAS Agile*, Elsevier, 2018, p. TBD.
- [8] Böhnke, D., Nagel, B., and Gollnick, V., “An approach to multi-fidelity in conceptual aircraft design in distributed design environments,” *32nd IEEE Aerospace Conference*, Big Sky, 2011.
- [9] Ciampa, P., Zill, T., and Nagel, B., “A hierarchical aeroelastic engine for the preliminary design and optimization of the flexible aircraft,” *54th AIAA/ASME/ASCE/AHS/ASC Structures, Structural Dynamics, and Materials Conference*, AIAA, 2013.
- [10] Vankan, W., Lammen, W., and Maas, R., “Meta-modeling and multi-objective optimization in aircraft Design,” *Advances in collaborative civil aeronautical multidisciplinary design optimization. Progress in Astronautics and Aeronautics*, Vol. 233, edited by E. Kessler and M. Guenov, American Institute of Aeronautics and Astronautics, 2010, Chap. 6.
- [11] Lammen, W., Kupijai, P., Kickenweitz, and Laudan, T., “Integrate engine manufacturer’s knowledge into the preliminary aircraft sizing process,” *Aircraft Engineering and Aerospace Technology: An International Journal*, Vol. 86, 2014, pp. 336–344.
- [12] MathWorks, T., “Matlab 2018,” , 2018. URL <http://www.mathworks.com>.
- [13] de Wit, A., “A Unified Approach towards Decomposition and Coordination for Multilevel Optimization,” Ph.D. thesis, Delft University of Technology, 2009.
- [14] Balling, R., and Sobieszczanski-Sobieski, J., “Optimization of coupled systems: A critical overview of approaches,” *AIAA Journal*, Vol. 34, 1996, pp. 6–17.
- [15] Martins, J., and Lambe, A., “Multidisciplinary design optimization: A survey of architectures,” *AIAA Journal*, Vol. 51, 2013, pp. 2049–2075.
- [16] Barthelemy, J., “Engineering design applications of multilevel optimization methods,” *Computer Aided Optimum Design of Structures: Applications*, 1989, pp. 113–122.
- [17] Wagner, T., “A general decomposition methodology for optimal system design,” Ph.D. thesis, The University of Michigan, 1993.

- [18] de Wit, A., and van Keulen, F., “Overview of Methods for Multi-Level and/or Multi-Disciplinary Optimization,” *51st AIAA/ASME/ASCE/AHS/ASC Structures, Structural Dynamics, and Materials Conference*, AIAA, 2010.
- [19] Tosserams, S., Etman, L., and Rooda, J., “Multi-modality in augmented Lagrangian coordination for distributed optimal design,” *Structural and Multidisciplinary Optimization*, Vol. 40, 2010, pp. 329–352.



Dedicated to innovation in aerospace

## Netherlands Aerospace Centre

NLR is a leading international research centre for aerospace. Bolstered by its multidisciplinary expertise and unrivalled research facilities, NLR provides innovative and integral solutions for the complex challenges in the aerospace sector.

NLR's activities span the full spectrum of Research Development Test & Evaluation (RDT & E). Given NLR's specialist knowledge and facilities, companies turn to NLR for validation, verification, qualification, simulation and evaluation. NLR thereby bridges the gap between research and practical applications, while working for both government and industry at home and abroad.

NLR stands for practical and innovative solutions, technical expertise and a long-term design vision. This allows NLR's cutting edge technology to find its way into successful aerospace programs of OEMs, including Airbus, Embraer and Pilatus. NLR contributes to (military) programs, such as ESA's IXV re-entry vehicle, the F-35, the Apache helicopter, and European programs, including SESAR and Clean Sky 2. Founded in 1919, and employing some 600 people, NLR achieved a turnover of 76 million euros in 2017, of which 81% derived from contract research, and the remaining from government funds.

For more information visit: [www.nlr.org](http://www.nlr.org)

### Postal address

PO Box 90592  
1006 BM Amsterdam, The Netherlands  
e ) [info@nlr.nl](mailto:info@nlr.nl) i ) [www.nlr.org](http://www.nlr.org)

### NLR Amsterdam

Anthony Fokkerweg 2  
1059 CM Amsterdam, The Netherlands  
p ) +31 88 511 3113

### NLR Marknesse

Voorsterweg 31  
8316 PR Marknesse, The Netherlands  
p ) +31 88 511 4444